First Cross-Section Observation of an All Solid-State Lithium-Ion "Nanobattery" by Transmission Electron Microscopy

A. Brazier,[†] L. Dupont,*[,†] L. Dantras-Laffont,[†] N. Kuwata,[‡] J. Kawamura,[‡] and J.-M. Tarascon[†]

LRCS−UMR 6007, Université de Picardie Jules Verne, 80039 Amiens, France, and Institute of Multidisciplinary Research for Advanced Materials, Tohoku University, Katahira 2-1-1, Aobaku, Sendai, 980-8577, Japan

Received November 29, 2007. Revised Manuscript Received January 14, 2008

Understanding and improving the behavior of interfaces is essential to the development of safer and high performance Li-based batteries regardless of their range of applications. Indirect methods such as impedance spectroscopy or direct methods such as the live in situ observation of batteries cycled within a scanning electron microscope (in situ SEM) are used to determine the interface microstructure/composition evolution upon cycling. These methods are used to establish a direct link between interface properties and batteries performance; they also enable us to spot local interface defects that are crucial to the development of 2D solid-state microbattery, for instance. Indeed, this technology is of interest in powering the new generation of microelectromechanical systems (MEMS). Here, we demonstrate the first ex situ TEM observation of "nanobatteries" obtained by cross-sectioning a microbattery using focus ion beam (FIB) in a dual beam SEM. Then, TEM analyses between pristine, cycled, and faulted all solid-state $LiCoO_2$/solid electrolyte/SnO Li-ion batteries have revealed drastic changes such as the presence, depending on the battery fabrication process, of both cavities within the solid electrolyte layers and low wetting points between the electrolyte and the negative electrode. Moreover, post-mortem TEM observations of cycled microbatteries have revealed a rapid deterioration of the interface upon cycling because of the migration of the chemical elements between stacked layers. Such findings are involved both in the improvement of the reliability of the 2D all solid-state battery assembling process and in the enhancement of their cycling performances. Such achievements constitute the technical platform for our future targets namely the development of live in situ TEM observation of "nanobatteries" cycled within the microscope.

Introduction

Nowadays, lithium-ion batteries are the heart of most portable electronic devices. This leadership is nested in the fact that lithium-ion batteries are light and could deliver a good volumetric energy over a great number of cycles. However, the Li-ion batteries suffer from safety limitations as illustrated by the recent incidents that have turned laptops into "flamethrowers". Enhancing safety is a must if one ever wants this technology to capture the electric transport market. At the opposite end of the energy storage spectrum are the solid-state microbatteries, whose performances and reliability are struggling to meet the energy demands dictated by the incoming generation of miniaturized autonomous devices such as MEMS. Much research is devoted to the aforementioned issues trying either to design new electrolyte additives to manufacture safer batteries on a large scale or to better understand interfaces to enhance the reliability and cycle-life of microbatteries. Besides impedance measurements, scanning electron microscopy (SEM) has proven to be a useful technique to study interfaces evolution such as, for instance, observing the Li plating stripping mechanism at the Li electrode/electrolyte interface either in an ex situ or in situ manner. Along that line, a few years ago we successfully modified an environmental SEM to perform in situ SEM studies of batteries cycling within the microscope chamber; this was done in order to monitor live and at the micrometer scale the lithium dendrite growth, the modification of the interfaces and the chemical species migration.[1,2]

Because of both the miniaturization of the power sources and the recent trend to move toward the utilization of nanomaterials and nanoarchitectured components, there is a need to observe smaller and smaller samples. Transmission electron microscopy (TEM) is known as one of the most powerful techniques to obtain structural, morphological and compositional information at nanometer scale by combining imaging, diffraction and spectroscopies (EDS and EELS). However, its use within the field of battery research has been mainly limited to the ex situ study of single and not assembled electrode components. Such studies mainly require the use of specifically designed sample holders capable of

* Corresponding author. Address: Laboratoire de Réactivité et de Chimie des Solides, 33 rue Saint Leu, 80039 Amiens Cedex, France. Fax: 322827590. E-mail: loic.dupont@sc.u-picardie.fr.
[†] Université de Picardie Jules Verne.
[‡] Tohoku University.

(1) Orsini, F.; du Pasquier, A.; Beaudoin, B.; Tarascon, J. M.; Trentin, M.; Langenhuigen, N.; de Beer, E.; Notten, P. *J. Power Sources* **1998**, *76*, 19–29.
(2) Orsini, F.; du Pasquier, A.; Beaudoin, B.; Tarascon, J. M.; Trentin, M.; Langenhuigen, N.; de Beer, E.; Notten, P. *J. Power Sources* **1999**, *81–82*, 918–921.

10.1021/cm7033933 CCC: $40.75
Published on Web 03/05/2008

protecting the sample from air exposure, thus enabling us to perform ex situ experiments. Therefore, one of the remaining key challenges and long-standing dreams for scientists working on lithium-ion batteries is to be able to observe, at the atomic scale and live, the interfaces evolution occurring in a battery while being cycled. Although the objective is clearly defined the obstacles to perform in situ TEM measurements are humongous owing to tricky technological problems linked to size, vacuum, etc.

It is needless to say that because of size considerations dictated by TEM studies, we must enter this field by first focusing on the miniaturized power sources (also called microbatteries) that are presently developed for microelectronic devices and integrated opto-electronic circuits. But, as-made microbatteries are still too thick to be directly observed by TEM, and therefore must be sliced to produce specimens amenable to the nanometer size required for transmission electron microscopy studies. Herein, we report our first successful ex situ TEM attempts to observe batteries interfaces. More precisely we will compare the interface evolution between a pristine and one cycled full "nanobattery" to highlight the benefits of such a characterization tool to spot interface defects, thus providing the key information to improve interfaces that will enhance the reliability and production quality of such micropower sources. The paper will be organized in three parts. First, the technical challenges that should be bypassed in order to successfully observe a lithium-ion battery in the TEM will be presented together with the solution we chose to break the technological locks. Afterward, the interest of our approach will be demonstrated through post-mortem analysis of pristine, cycled, and faulty microbatteries. Finally, in light of such promising results, the essential remaining steps leading to a full in situ observation, which are actually being tackled, will be given as perspectives.

Results and Discussion

"Nanobattery" Preparation. The term nanobattery refers to the thickness of the all solid-state battery that we should prepare to realize a TEM observation. Indeed, since all solid-state batteries having a thickness in the range of the micrometer are called microbattery, thin TEM cross-sections of these batteries (a few nanometres thick) will be called nanobatteries.

The vacuum ruling in the TEM column bans the use of liquid or polymer battery technologies so that the all solid-state thin film batteries are presently the sole candidates for such microscopy studies. Going from an all solid-state battery to the suitable nanobattery required for TEM observation is a tedious process involving several steps such as the assembly of the microbattery, its cross-section as well as the mounting of the resulting nanobattery into the microscope. The details are as follows.

1. Preparation of an All Solid-State Microbattery. Such a battery consists of a multilayered stacking, comprising the positive and negative electrodes, the electrolyte and some additional layers such as current collectors, all in a solid state. There are several techniques to separately manufacture the different components of the thin film batteries. Vacuum thermal vapor deposition is generally used for the metallic lithium deposition as negative electrode together with chemical vapor deposition,[3] RF sputtering,[4] RF magnetron sputtering, or molecular beam deposition[5] for components materials of oxide for the positive electrode or electrolyte. For the lithium-ion thin film batteries, in addition to the previous techniques, pulsed laser deposition (PLD) is also commonly used, especially for the positive electrode materials. This deposition process is a well-known relevant technique to obtain films of same composition as the target and good surface morphologies, enabling us to get good stacking. Regarding the negative electrode, most of the existing devices are using metallic lithium that at first, should be avoided in order to facilitate the preparation of the cross-section; the reason being two-fold. First, lithium is a soft material that could slobber over the other layers during the preparation. Second, its strong moisture sensitivity prevents any manipulation in ambient environment. Keeping this in mind, all solid-state Li-ion batteries made by PLD technique and developed by Kuwata et al.[6,7] were selected for our experiments. These microbatteries are deposited on glass substrates using the design shown on Figure 1a, including (1) Pt/Cr positive electrode current collector, (2) $LiCoO_2$ positive electrode, (3) amorphous Li_2O-V_2O_5-SiO_2 (LVSO) solid electrolyte, (4) SnO anode, and (5) Pt negative electrode current collector. Typically, the batteries have a surface of about 0.23 cm^2 (Figure 1b) and are about 3.5−4 μm thick. All fabrication steps and characteristics of the batteries have been previously reported.[6,7] LVSO was selected because of its easy synthesis method, its good electrolytic characteristics (ionic conductivity 3×10^{-7} S cm^{-1}; good electrochemical stability window). Moreover, good quality thin films could be obtained using a pulsed laser deposition technique (smooth, dense, without any pinhole or cracks).[6] SnO was chosen as a good alternate to lithium as negative electrode because it presents a higher stability against humidity, a low potential, and a good cyclability thanks to the reversible alloying process between metallic tin and lithium.

2. Cross-Section of the Microbattery. To observe an entire microbattery in TEM in high-resolution, it is mandatory to thin down our specimen to reach a very small thickness, less than 50 nm, for the electrons to go through. Many preparation techniques exist, namely ion milling or ultramicrotomy, in order to perform cross-sections, but they both require the use of solvents. Because of both the lithiated nature of the materials inside our battery and the risks of short-circuit, all the conventional cross-section techniques must be banished. On the opposite, focused ion beam, commonly used for microfabrication,[8] selective materials deposition or sample polishing, has been found to be a relevant technique to bypass

(3) Kanehori, K.; Ito, Y.; Kirino, F.; Miyauchi, K.; Kudo, T. *Solid State Ionics* **1986**, *18–19*, 818–822.
(4) Neudecker, B. J.; Zuhr, R. A.; Robertson, J. D.; Bates, J. B. *J. Electrochem. Soc.* **1998**, *145*, 4160–4168.
(5) Birke, P.; Chu, W. F.; Weppner, W. *Solid State Ionics* **1996**, *93*, 1–15.
(6) Kuwata, N.; Kawamura, J.; Toribami, K.; Hattori, T.; Sata, N. *Electrochem. Commun.* **2004**, *6*, 417–421.
(7) Kuwata, N.; Kumar, R.; Toribami, K.; Suzuki, T.; Hattori, T.; Kawamura, J. *Solid State Ionics* **2006**, *177*, 2827–2832.
(8) Vasile, M. J.; Nassar, R.; Xie, J.; Guo, H. *Micron* **1999**, *30*, 235–244.

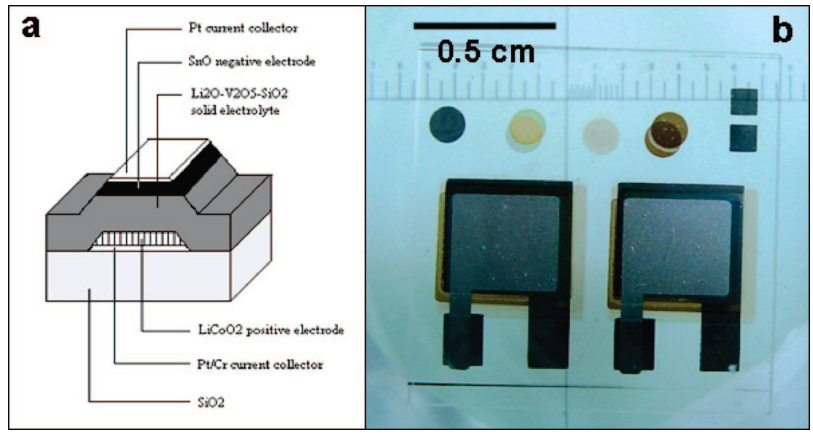

Figure 1. (a) Schematic view of the microbattery developed stacking sequence. (b) Top view of two microbatteries (area ≈ 0.23 cm^2) deposited at the same time on the same glass substrate.

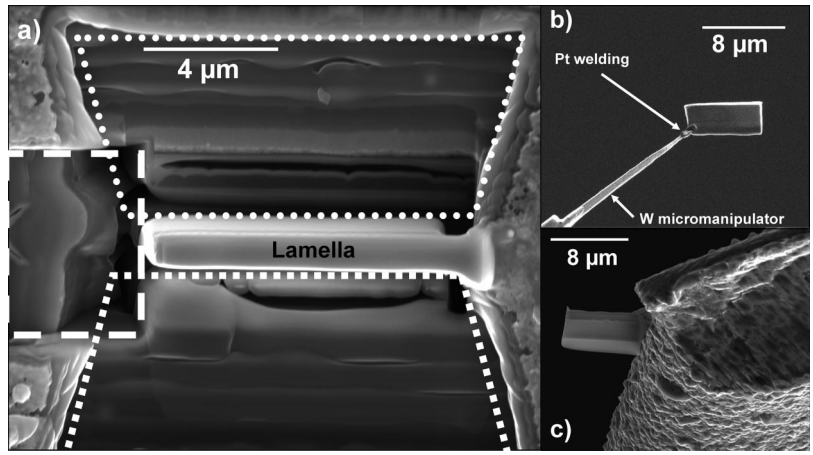

Figure 2. (a) Focused ion beam secondary electron image of the TEM specimen before lifting it out: the bottom, left side, and a portion of the right side are cut free (dashed line regions). (b) The specimen is "lifted out" from the bulk sample and (c) welded on a standard Cu TEM grid.

these problems; it can also be adapted to slice multilayer devices (Loos et al.) for the preparation of a cross-sectional sample of a polymer solar cell deposited on glass substrates.[9]

FIB operates in a dual beam SEM (one conventional electron beam + one gallium ion beam). Using both beams, images could be created, thanks to the secondary electrons or ions ejected from the observed material, while the interest of the gallium beam is the sample cutting and thinning with very high accuracy: the used ions can be focused on a very fine probe size (<10 nm).[10] Moreover, this technique does not require any pretreatment of the sample. The beam being quite energetic, a thin Pt layer is deposited by a micro-injector on the top of the device, forming a local surface where the specimen will be removed from, in order to avoid the amorphization of the top layer.[10] Inside the SEM, two sides of the area of interest are cut as seen on Figure 2a; a large staircase trench is cut on one side and a rectangular trench on the other side (dashed line delimiting the excavated regions). The resulting wall will become the cross-section lamella having parallel faces. Then the sample is tilted in order to cut the bottom, the left side and a part of the right side, free (Figure 2a). The sample is tilted back to its original position. A tungsten manipulator is welded (with the Pt of the micro-injector) on the free part of the sample (Figure 2b) and the right part is then cut free. This in situ process is used to transfer the thin membrane onto a copper TEM grid, where the sample is welded with Pt (Figure 2c). The ion beam is once again used to thin the sample in order to obtain a convenient thickness of about 100 nm with a routine thinning; but it can be reduced to about 40 nm using a low voltage and a low current machine process at the end of the cutting. The pristine and cycled microbatteries cross-sections described below were subjected to the latter. At this stage, due to the thickness of the cross-section (in the nanometer range), the obtained battery is called nanobattery.

3. Setup of the Nanobattery in the Microscope. The last step, prior to TEM investigation, concerns the transfer of the sample from the Dual Beam SEM to the TEM. The welding of the nanobattery on a special TEM copper grid makes its installation on any type of TEM holder easy; the latter should then be placed into a microscope. Ideally, for fully charged cells (i.e., having no free metallic Li remaining and a free Li containing negative electrode), such a transfer could at first sight take place in a non controlled environment. However, such a way of operating prevents the observation

(9) Loos, J.; van Duren, J. K. J.; Morrissey, F.; Janssen, R. A. J. *Polymer* **2002**, *43*, 7493–7496.
(10) Giannuzzi, L. A.; Stevie, F. A. *Micron* **1999**, *30*, 197–204.

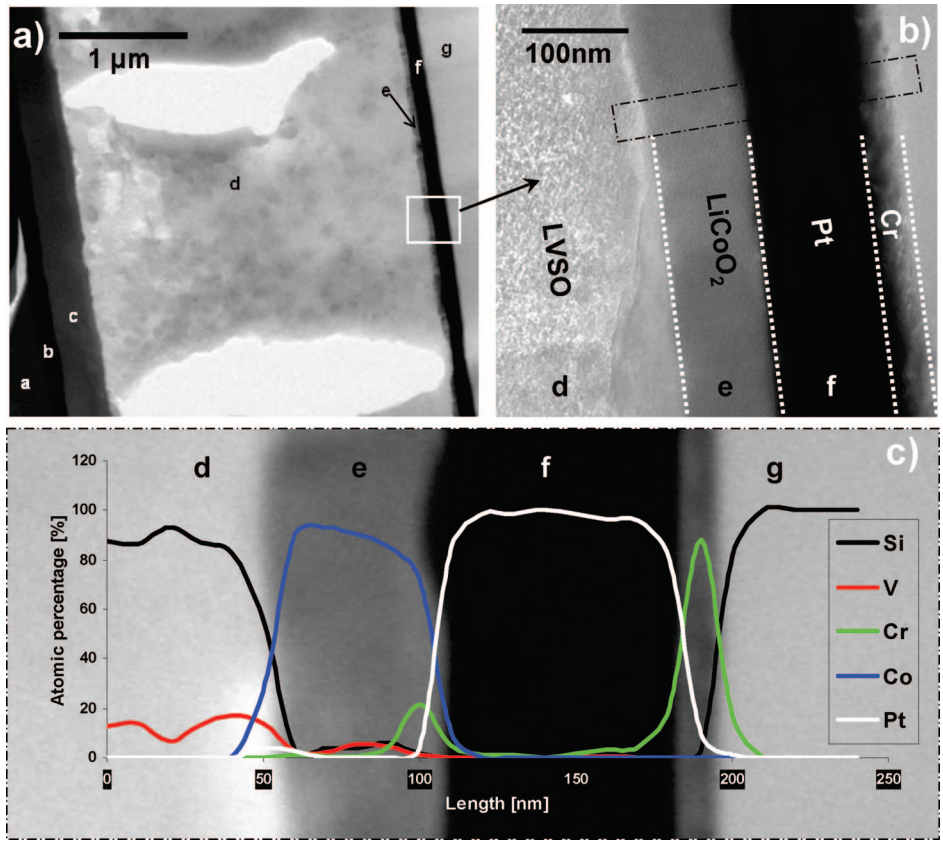

Figure 3. (a) TEM image of the entire structure of a pristine microbattery showing the following sequence: (a) FIB deposited platinum/(b) PLD platinum/(c) SnO/(d) LVSO electrolyte/(e) $LiCoO_2$/(f) PLD chromium and platinum, and (g) glass substrate. (b) TEM image at higher magnification of the region close to the $LiCoO_2$ positive electrode. (c) EDS line profile analysis by STEM.

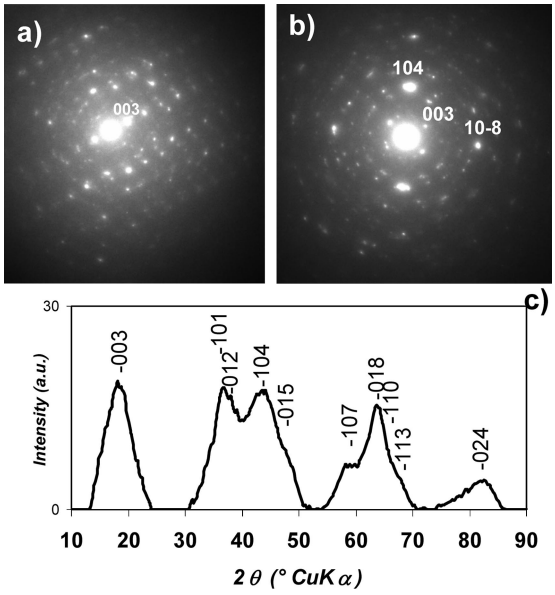

Figure 4. (a, b) Selected area electron diffraction (SAED) patterns of the pristine $LiCoO_2$ layer. (c) Process diffraction treatment of the SAED pattern shown in (a).

of partially discharged or charged cells. To bypass this issue, our team has (1) already modified an air lock system to transfer samples from an adapted SEM chamber to the inert atmosphere of a glovebox[11] where the grid could be mounted, moisture-free, on a TEM holder, and (2) created a specific system that could enable to place the TEM holder into the microscope without any air exposure.[11] All of the following TEM analyses were carried out using a STEM TECNAI F20 S-Twin operating at 200 kV and equipped with Energy Dispersive Spectroscopy (EDS) analysis capabilities.

Observations of Nanobatteries. Having described how our studied "nanobatteries" have been obtained, we will show our way of monitoring by TEM the evolution of the various layers and interfaces constituting the nanobattery both as a function of cycling and of the assembling process. For our measurements to be meaningful, two microbatteries (Figure 1b) were made at the same time, according to the aforementioned standard procedure and on the same glass substrate, so we can assume that they are identical except for homogeneity problems linked to our depositing process. Owing to such duplication, the cycled microbattery will always be compared to the pristine one to rapidly spot the cycling-induced differences. Establishing such comparisons will enable us to understand not only why some microbatteries are faulty once made, and therefore cannot be cycled, or why some cells fail after a few cycles. Such information will be used to modify or correct the assembling process of microbatteries and enhance its reliability. Both cases are now presented through the following examples.

1. Pristine. The cross-section bright-field (BF) TEM images of a pristine microbattery are shown on Figure 3. Because of the observed change in contrast on the micrograph, the numerous stacked layers constituting the battery

(11) Orsini, F.; Dupont, L.; Beaudoin, B.; Grugeon, S.; Tarascon, J.-M. *Int. J. Inorg. Mater.* **2000**, *2*, 701–715.

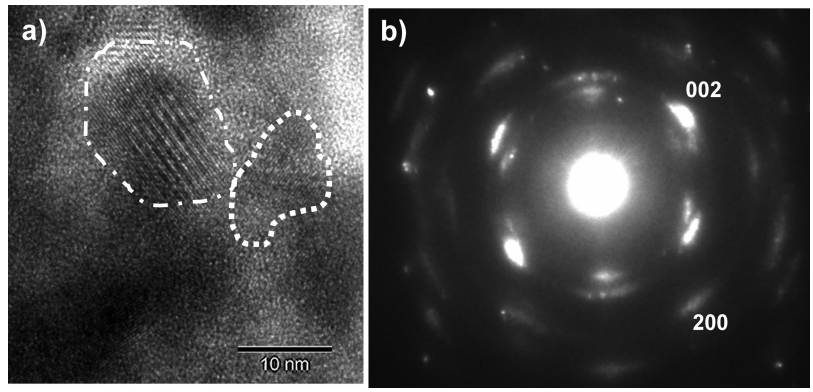

Figure 5. (a) HRTEM micrograph of the SnO layer and (b) the corresponding SAED pattern.

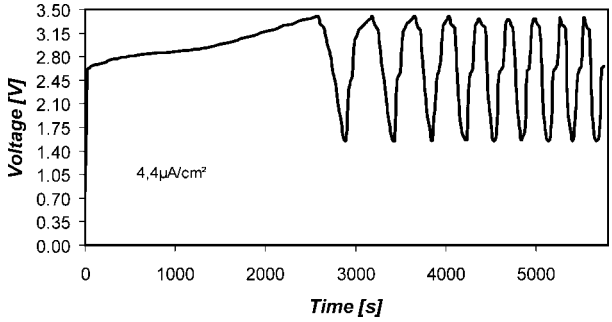

Figure 6. Charge–discharge profiles over 10 galvanostatic cycles ($i = 4.4$ μA cm^{-2}) of the microbattery.

are easily identified with letters (from a to g) corresponding to the following sequence: (a) FIB deposited platinum, (b) PLD platinum, (c) SnO deposit, (d) LVSO electrolyte, (e) $LiCoO_2$ layer, (f) PLD chromium and platinum, and (g) glass substrate. Letters ranging from a to g will be added on each TEM micrograph as soon as the corresponding layer is displayed. At higher magnification, the distinction between PLD platinum and chromium layers is spectacular (Figure 3b). It is worth noting that the layer sequence established through visual observation was confirmed by EDS line profile analysis using the STEM capability as partially shown on Figure 3c. Indeed, the evolution of the chemical composition could be nicely monitored using this technique. Moreover, both BF image and EDS line profile analysis evidence that the interfaces between all layers are quite thin and well-defined. Moreover, it is worth mentioning that there are neither any significant element migrations between the concerned layers during the preparation process of the nano-battery nor any notable gallium implantation during the cutting. The same analysis has been performed close to the SnO negative electrode (not given in this study), showing again an obvious separation between the layers and no significant migration.

To go further and fully characterize the pristine "nano-battery", we are now detailing the morphology and composition of all layers constituting its electrochemically active part together with the electrolyte.

(a) $LiCoO_2$ Layer. The selective area electron diffraction (SAED) pattern and the corresponding XRD-like diagram first show that the 60 nm PLD deposited $LiCoO_2$ layer is crystallized (Figure 4). The observed reflections could be indexed using the high temperature lamellar $LiCoO_2$ cell parameters ($R\bar{3}m$ α-$NaFeO_2$ layered structure). Moreover, no preferential orientation is observed as, for instance, the (104), (10$\bar{8}$), and (003) directions are observed on the same SAED pattern, showing that the grains forming the layer are small and randomly distributed.

(b) LVSO Layer. As expected, the EDS spectrum of the electrolytic film, whose width is about 2.7 μm, shows the presence of vanadium, silicon (Figure 3c), and oxygen (not shown on the line profile). The SAED pattern is featureless confirming its amorphous structure.[6,7] Attempts to obtain the thinnest cross-sections for TEM observation resulted in the appearance of elliptic shape cavities perpendicular to the stacking and having their maximum width in the middle of the layer. Either the torsion of the slice during the machining or the redeposition effect implying a non homogeneous attack (Figure 3a) could be at the origin of these cavities.

(c) SnO layer. The negative electrode has a width of about 340 nm and is made of 10 nm well crystallized grains as deduced from HRTEM images, which clearly show atomic layers (Figure 5a). The corresponding SAED pattern shows dots that could be indexed according to SnO cell parameters (Figure 5b).

2. Cycled Battery. While the first microbattery (pristine) was sliced for a TEM observation of the cross-section, its twin (Figure 1b) was cycled using a galvanostatic method ($i = 4.4$ μA cm^{-2}) over 10 cycles. We note a humongous irreversible capacity between the first charge and discharge. Moreover, the capacity rapidly fades upon cycling (Figure 6). The molar ratio $LiCoO_2$/SnO (not calculated but estimated from the thicknesses of the films) is definitely too small to compensate for the irreversible capacity due to the formation of Li_2O at the first charge ($SnO + 6.4Li \rightarrow Li_2O + Li_{4,4}Sn$).[7] Rather than trying to obtain the best cycling battery from several assembling trials, we decided to pursue the investigation of such a poor performing cell in order to first demonstrate the feasibility to cross-section our microbattery, and perform post-mortem observations at the nano scale. Moreover, performing our first TEM investigations on such a poorly performing battery was ideal to see how useful the technique could be in providing materials/interfaces information that could explain its rapid cycling decay.

The TEM cross-section images of the cycled battery are given in Figure 7. From the entire view (Figure 7a) it is very difficult to differentiate between the layers composing the stacking, except for the platinum current collectors, which

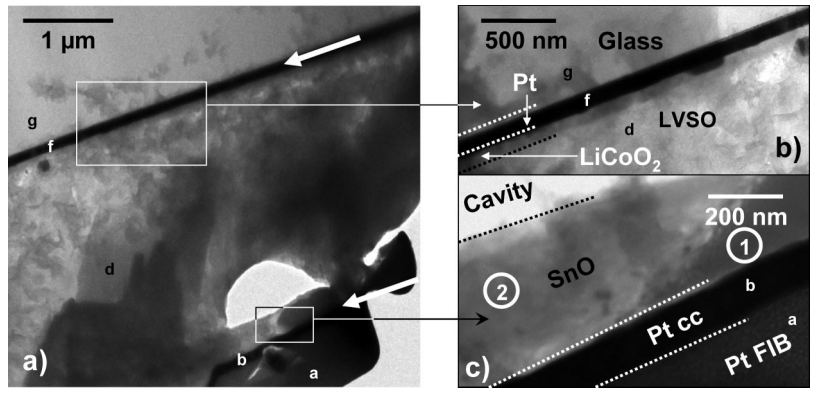

Figure 7. (a) TEM image of the cycled microbattery. The arrows indicate the positive (top) and the negative (bottom) Pt current collectors layers. (b, c) Higher-magnification images of the $LiCoO_2$ positive electrode region and SnO negative electrode region, respectively.

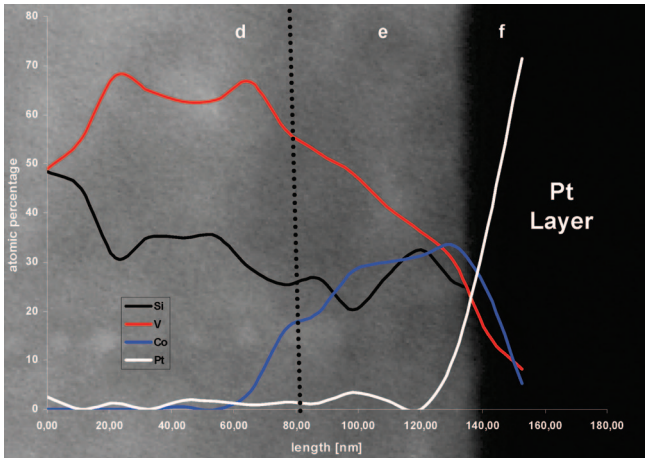

Figure 8. EDS Line profile analysis by STEM of the region near the $LiCoO_2$ positive electrode of a cycled microbattery.

are darker than the other layers (white arrows on the figure). Even by higher resolution near the current collectors (images b and c in Figure 7), it is quite difficult to see the difference between LVSO and both $LiCoO_2$ and SnO. On the positive electrode side (Figure 7b), a weak contrast modification enables to hardly distinguish the $LiCoO_2$ layer from the LVSO electrolyte. On the negative electrode side (Figure 7c), a contrast variation is locally observed within the layer where the tin oxide should be. A number labels each region which will be analyzed by EDS as detailed below. Overall, it looks as if the structure is destroyed upon cycling, and the first assumption for the layer "disappearance" in our images is rooted in chemical elements migrations, hence reducing the Z contrast between each layer. Like for the pristine microbattery, a STEM line profile analysis has been performed close to the $LiCoO_2$ electrode to highlight the species migration (Figure 8). There is still a region where the Co amount is important, corresponding to the region where $LiCoO_2$ layer should be, with a width of about 60 nm (cf. the reference microbattery on Figure 3c). But the atomic profile also reveals an important quantity of silicon and vanadium in this layer. Likewise, cobalt is also detected within the LVSO electrolyte. Such results unambiguously account for a well-pronounced migration of the chemical element between the $LiCoO_2$ and the LVSO layers so that the initial well-defined interface is no longer preserved upon cycling.

Turning to the SnO layer, a line profile analysis (not shown here) at the interface of the two regions with a different contrast (called region 1 and 2, Figure 7c) shows that region 1 is only composed of Sn and O, whereas region 2 is a mix of Sn, O, V, and Si, confirming once again the migration of Si and V from the LVSO electrolyte to the SnO negative electrode during the cycling. So, how can we explain the presence of these two distinct regions? We assumed that the cavities appeared during FIB cutting; however, even if this technique has intensified the presence of these cavities; the shape of the ones close to the negative electrode (Figure 7a) are quite unusual as one side of the hole is linear and parallel to the platinum current collector. The distance between the edge and the platinum corresponds to the thickness of the initial SnO layer. Consequently, we believe that part of the SnO layer was previously delaminated from the LVSO layer so that region 1 will behave as electrochemically dead matter. The presence of the electrochemically inactive regions of the SnO electrodes could simply explain the poor use of the negative electrode and its reduced use during the discharge; hence the large observed difference between the first charge and discharge capacity. Because of the presence of these inactive regions, the large charge capacity should imply the presence of Li plating at the negative electrode; we could not detect any evidence for such extra deposits.

3. Faulty Microbattery. We sometimes experienced difficulties in cycling the pristine battery and more especially so at the early stage of the project when the PLD technique and the assembly process of the all solid-state battery were not fully mastered yet. Here again the post-mortem study of such "dead" microbattery through the cross-section observation by TEM turned out to be quite useful, as demonstrated below, in determining the key parameters to be corrected to enhance the device building process quality.

The low-resolution TEM images of the faulty battery (images a and b in Figure 9) shows the different layers (see contrast differences) for which the deposition times have been changed to modify the films thicknesses. The layers have now the following widths: Pt, 100 nm; SnO, 150 nm; LVSO, 1750 nm; $LiCoO_2$, 250 nm; Pt/Cr, 140 nm. The sample is a rectangular thin slice (8 μm $\times$ 4 μm and around 100 nm thick).

On Figure 9b, a defect, characterized by a thin darker layer parallel to the others and denoted by the white arrow, can

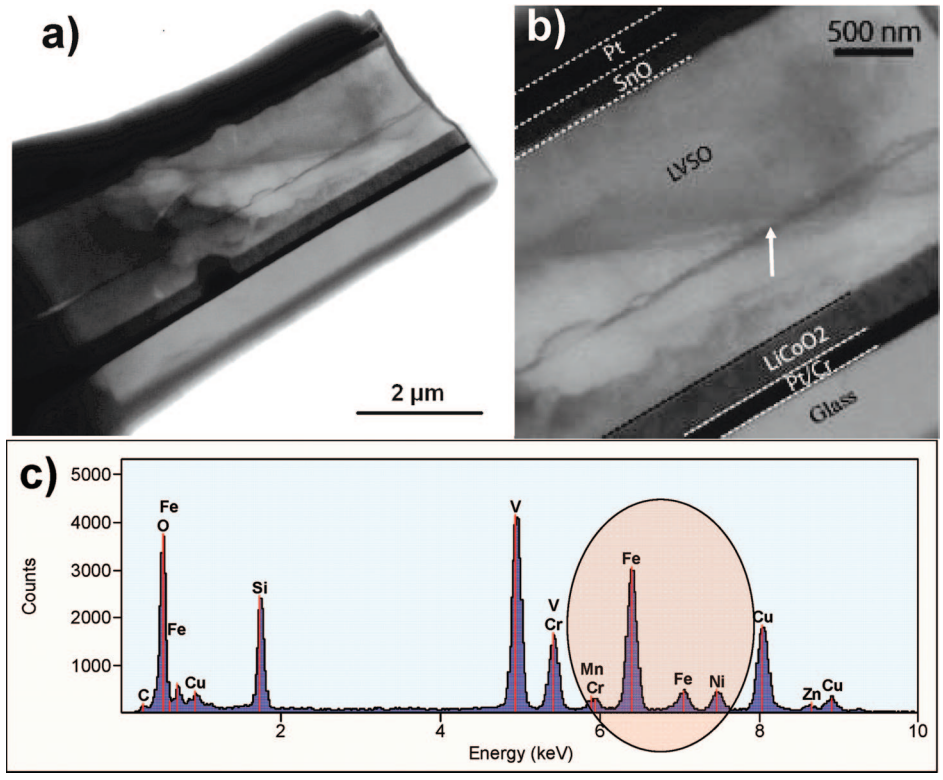

Figure 9. (a, b) TEM images of a faulty microbattery. The arrow in (b) indicates the undesirable layer. (c) EDX spectrum of the undesirable layer.

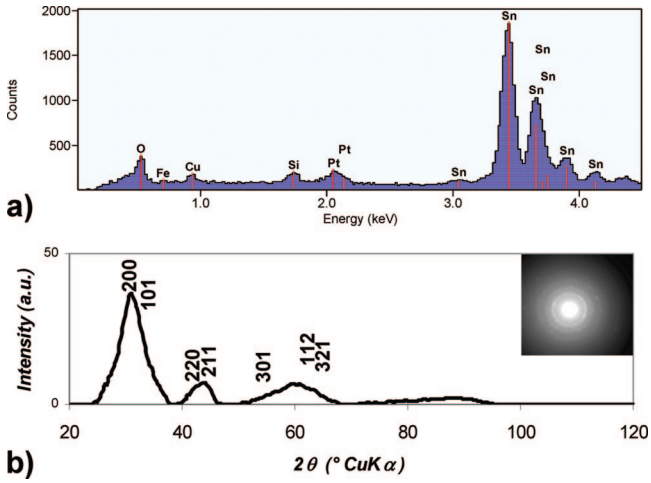

Figure 10. (a) EDX spectrum of the negative electrode of the faulty microbattery. (b) Process diffraction treatment of the SAED pattern shown inset.

be spotted in the middle of the LVSO film. Its EDS analysis indicates the presence of iron, nickel, and chromium. Such an undesirable layer, which appeared while depositing the LVSO layer, was obviously due to the ablation of the stainless steel target holder because of a poor positioning of the target with respect to the laser plume. Such a layer may prevent the ion transfer between both electrodes, then accounting for the inability to electrochemically activate the cell.

Besides this unexpected foreign layer, we also note that the negative "SnO" electrode was quite deficient in oxygen, as deduced by the EDS spectrum, which barely shows the presence of an oxygen signal (Figure 10a). The assumption was further confirmed by the SAED pattern (Figure 10b) since the corresponding XRD-like diagram could be indexed by solely using metallic tin cell parameters. Because of such finding, the partial pressure of oxygen within the laser deposition chamber has been tuned differently.

The characterization of such a faulty microbattery specimen shows how powerful this observation technique is to determine the origin of the deposition process problems. This technique easily permits us to control the reliability of such device from a morphological point of view.

Conclusions

The focused ion beam technique was successfully used to obtain for the first time thin cross-sectioned nanobattery samples out of a solid-state microbattery; they were studied by TEM microscopy in an ex situ mode to determine the origin of both the high percentage rate of faulty assembled batteries and of the microbattery capacity fading upon cycling. The comparison between one cycled and one pristine microbattery sliced by FIB and observed by TEM and STEM allowed us to clearly demonstrate chemical elements migration between the electrolyte and both the positive and negative electrodes, together with the partial use of the SnO negative electrode due to delaminating of the layers.

At this stage, such post-mortem observation provides key information sorely needed for the control and improvement of microbattery assembly as well as on the understanding of the electrochemical mechanisms governing this new type of device. Undoubtedly, nanobattery TEM observation will be one of the key techniques leading to a fast development of commercial 2D or 3D all solid-state microbatteries that could, in the near future, be integrated in radio-frequency

identification (RFID) tags or could replace the massive coin cell on integrated printed circuit boards.

Although the above ex situ TEM observations of nanobatteries have provided crucial information, they cannot presently be carried out at the various states of charge or discharge, due in such special cases to the reactivity of the negative electrode materials under ambient atmosphere. Hence our motivation to develop an experimental setup enabling to cycle a nanobattery within the microscope while performing live in situ TEM observations. Besides the ways to handle such a nanobattery in a moisture-free environment, one of the remaining challenges is to find ways to connect the "nanobattery" current collectors to an outside power supply capable of delivering very small current so as to limit the charge/discharging current densities. We are presently developing a power supply unit that could accurately deliver currents as low as 1 pA, corresponding to a drain current density of 100 μA cm^{-2} for a 100 nm $\times$ 10 μm "nanobattery".

Acknowledgment. L.D. thanks the Région Picardie for an "Appui à l'Emergence" (Emergence Support) studentship for A.B. L.D. thanks Alistore Network for the financial support and FEI Company, especially Hans Kempeneers, for the free access to the FIB.

CM7033933